Thermochimica Acta 494 (2009) 71–79

Contents lists available at ScienceDirect

Thermochimica Acta

journal homepage: www.elsevier.com/locate/tca

# Improvement of the thermal diffusivity measurement of thin samples by the flash method

Kuk-Hee Lim [a], Seog-Kwang Kim [b,*], Myung-Kyoon Chung [a]

[a] Department of Mechanical Engineering, Korea Advanced Institute of Science and Technology, 335, Gwahangno, Yuseong-gu, Daejeon 305-701, Republic of Korea
[b] Thermophysical Property Lab., Korea Advanced Institute of Science and Technology, 335, Gwahangno, Yuseong-gu, Daejeon 305-701, Republic of Korea

ARTICLE INFO

*Article history:*
Received 2 February 2009
Received in revised form 2 April 2009
Accepted 22 April 2009
Available online 3 May 2009

*Keywords:*
Flash method
Thermal diffusivity
Graphite coating
3-Layer model
Flash pulse width

ABSTRACT

In the conventional thermal diffusivity measurement by the flash method, the effect of finite width of the flash pulse and the effect of graphite layers on both front and rear surfaces are often neglected. In the present study, the error of the half-time method caused by the graphite layers is theoretically assessed and the minimum thickness ratio required for accurate measurement by the half-time method is investigated. In order to minimize the error of the flash method in measuring the thermal diffusivity of a thin sample coated by graphite, 3-layer model is proposed that includes corrections of the finite pulse effect and the heat loss effect. The proposed model is applied to measure the thermal diffusivities of copper, aluminum, iron and Inconel 600. It is found that the proposed 3-layer model reduces the measurement error considerably.



## 1. Introduction

The flash method is one of several methods to measure thermal diffusivity of various solid materials [1]. Since the preparation of the material specimen is simple, measurement time is relatively short, and measurement accuracy is in many cases good, it has been widely used in industries and research institutions. The conventional flash method is based on the fact that the thermal diffusivity is a simple function of the sample thickness and the half-time $t_{1/2}$ that is the time elapsed from the flash pulse heating to the time where the rear surface temperature reaches half of its maximum. Such relation is theoretically obtained under assumptions that there is no heat loss from the sample specimen to its surrounding, there are no coating layers of any type, and heating flash pulse is width-less and uniform. However, the assumed conditions are only ideal, and deviation of the real situation from these assumptions leads to inaccuracy of the thermal diffusivity measurement. Errors caused by these deviations have been theoretically and experimentally studied worldwide such as: radiation heat loss effect [2–5], non-uniform heating effect [6,7], graphite coating effect [8–13] and finite pulse time effect [14–16], etc.

Finite pulse time effect caused by the actual pulse of finite width must be corrected if the response time of the transient temperature rise curve is very short. For this study, an adequate time dependent function must be employed to represent the variation of the light intensity with time during the pulse heating. It is known that the pulse shape of the laser or xenon flash is well described by an exponential function [14]. Realistic pulse shape can be obtained by controlling the number of the time constants in the exponential function [16].

In the flash method, both front and rear surfaces are often coated with a thin, opaque and black layer, usually a graphite layer to increase the absorbance of flash energy at the front surface as well as to increase the emissivity at the rear surface so that the surface temperature may be easily detected by the IR-detector. Since the graphite layer is usually very thin, its thermal resistance is negligible if the sample has an adequate thickness. In the cases when the sample is relatively thin or the sample material is highly conductive, however, thermal resistance effect of the coating layer must be considered to determine the thermal diffusivity accurately. Unfortunately, however, since it is difficult to measure the thickness and the thermo-physical properties of the graphite coating layer [8], it is not easy to estimate the graphite coating effect quantitatively. There appeared a few researches to evaluate the thermal resistance of the graphite coating layer, but reliable data are not yet available. Araki et al. [10] attempted theoretically to evaluate errors caused by the graphite coating for a one-side coated sample using thermal properties of the graphite coating which had been experimentally determined by a 2-layer model.

Guo et al. [11] used the thermophysical properties of graphite from TPRC data book [17] to evaluate the thermal diffusivity of a thin diamond film by using a 3-layer model. In a 3-layer model

* Corresponding author. Tel.: +82 42 350 5066; fax: +82 42 350 2370.
*E-mail address:* skwang@kaist.ac.kr (S.-K. Kim).

0040-6031/$ – see front matter © 2009 Elsevier B.V. All rights reserved.
doi:10.1016/j.tca.2009.04.019

of Cernuschi et al. [12], they estimated the thermal diffusivity of graphite coating by using the Voigt–Reuss model with tabulated known values of thermophysical properties of graphite. The Voigt–Reuss model assumes that the graphite grains and voids are stacked like a column. But the graphite grains are usually stacked randomly, and the Voigt–Reuss model is therefore not correct.

On the other hand, in order to take the graphite coating effect into account, Kim and Kim [13] have developed a noble method to determine the thermal diffusivity by introducing an apparent thickness of the graphite coating layer. Scrutinizing a large number of transient temperature rise curves at the rear surface of various sample materials, they found an empirical correlation that relates the apparent thickness of the graphite coating layer to the delayed half-time. They added the apparent thickness found in this way to the sample thickness in the 1-layer model to determine the thermal diffusivity. But, since the empirical correlation has been obtained for a limited range of half-time, when the measured half-time is very short, their method often leads to erroneous evaluation of the thermal diffusivity. Moreover, they did not consider the change of the half-time caused by the finite pulse time effect and heat loss effect.

In the first part of the present work, apparent thermal diffusivity is defined for the 1-layer model, and the relation between the apparent thermal diffusivity and the thickness ratio $L^* = L_s/L_{gr}$ (sample thickness/graphite coating thickness) is investigated with the specific thermal mass ratio $(\rho C)^* = (\rho C)_s/(\rho C)_{gr}$ as a parameter. In this study, two cases are considered. One is that only the sample thickness is used in the 1-layer model, and the other case is that the thickness of the graphite layers is added to the sample thickness in the evaluation of the thermal diffusivity. From this study, minimum sample thickness required to secure accurate thermal diffusivity is obtained.

In the second part, in order to propose a 3-layer model that treats the effect of the graphite coating layer explicitly, the thermophysical properties of the graphite itself are measured. In the final part, in order to assess the reliability of the proposed 3-layer model and to investigate the finite pulse time effect, quantitatively, transient temperature rise curves for a total of four typical metal samples are measured and both 1-layer model and 3-layer model are applied to evaluate the thermal diffusivity. In these test measurements, the effect of the finite pulse time correction on the measurement accuracy will also be investigated.

## 2. Apparent thermal diffusivity

The fundamental principle of the conventional flash method to measure the thermal diffusivity of a 1-layer sample is that the thermal diffusivity is a function of the half-time $t_{1/2}$, the time elapsed from the pulse heating to the time when the rear surface temperature reaches half of its maximum temperature rise. The thermal diffusivity by the half-time method [1] for a 1-layer sample is evaluated from the following equation:

$$\alpha = \frac{0.1388L^2}{t_{1/2}} \tag{1}$$

Here $L$ is the thickness of the sample. This equation is accurate only when the following conditions are satisfied [5]: (a) the light pulse width is negligibly short, (b) heating by the flash light is uniform over the front surface of the sample, (c) there is no heat loss during measurement after pulse heating, (d) the sample material is uniform and homogenous and (e) the sample is nontransparent to the light pulse.

When the flash method is applied to measure the thermal diffusivity of a sample that is coated with graphite layers at both sides, if the sample thickness is sufficiently thick, the thermal resistance of the graphite coating layers is usually neglected and the coated sample is assumed as a homogeneous material. If the graphite coating layer is not negligible, the thermal resistance of the graphite coating layers must be explicitly considered. For such a 3-layered structure, the effective thermal diffusivity can be calculated by the following equation:

$$\alpha_e = \frac{(L_s + 2L_{gr})^2}{(L_s/\alpha_s(\rho C)_s) + 2(L_{gr}/\alpha_{gr}(\rho C)_{gr})\{(\rho C)_s L_s + 2(\rho C)_{gr} L_{gr}\}} \tag{2}$$

Here $(\rho C)$ is specific thermal mass, $\rho$: density, $C$: specific heat and subscript $s$ and $gr$ indicate the sample and the graphite coating layer, respectively. Even though the thermophysical properties of the graphite coating are known a priori, since generally there is no way to directly measure the effective thermal diffusivity, the thermal diffusivity of the sample material cannot be obtained by Eq. (2).

Since the matching condition of heat flux at each interface between the adjacent layers must be satisfied, the temperature rise at the rear surface for a multi-layered structure is quite different from that of a homogenous single layer. Consequently, if the half-time $t_{1/2}$ actually measured from the multi-layered material is substituted into Eq. (1) for a 1-layer sample, the resulting thermal diffusivity is neither the effective nor the true thermal diffusivity of the sample. It is only an apparent value of the thermal diffusivity of the sample material. Hence, it is called "apparent thermal diffusivity ($\alpha_{apparent}$)" in the present study. When $\alpha_{apparent}$ is calculated by Eq. (1), depending on whether the graphite coating layers are included or not in the sample thickness $L$, we consider the following two cases:

$$\text{Case ①};\quad L = L_s$$

$$\text{Case ②};\quad L = L_s + 2L_{gr} \tag{3}$$

In order to investigate the error caused by the presence of the graphite coating layers, the unsteady heat conduction equation is numerically solved with appropriate boundary conditions and $\alpha_{apparent}/\alpha_{gr}$ is calculated theoretically as a function of the thickness ratio $L^* = L_s/L_{gr}$ with the specific thermal mass $(\rho C)^* = (\rho C)_s/(\rho C)_{gr}$ as another parameter. A total of six materials are considered. They are: $\alpha^* = \alpha_s/\alpha_{gr} = 0.01$, 0.1, 1, 10, 100, and 1000. Fig. 1 represents the results for both Cases ① and ② . As can be seen from the figures, $\alpha_{apparent}$ determined by Case ① is always less than $\alpha_s$ and the value asymptotes to the accurate thermal diffusivity $\alpha_s$ as the thickness ratio becomes large. The effect of the specific thermal mass ratio is found to be significant especially when the thermal diffusivity ratio is less than one (Fig. 1(a) and (b)). This result shows that the sample must be sufficiently thick when both ratios of the thermal diffusivity and the specific thermal mass are less than one.

If the graphite thickness is added to the sample thickness when the apparent thermal diffusivity is evaluated (Case ② ), Fig. 1 shows that the measured $\alpha_{apparent}$ approaches to the thermal diffusivity of the graphite itself for small $L^*$, whereas it asymptotes to the sample's true thermal diffusivity for large $L^*$. In summary, If $\alpha^*$ is less than or equal to 1, $\alpha_{apparent}$ is sensitive to both $L^*$ and $(\rho C)^*$ while it is sensitive only to $L^*$ for $\alpha^* > 1$. As $L^*$ is decreased, $\alpha^*$ converges to 0 in Case ① since $L_s \approx 0$. But it converges to 1 in Case ② since $L = L_s + 2L_{gr} \approx 2L_{gr}$. As $L^*$ is increased, $\alpha_{apparent}/\alpha_{gr}$ converges to the assumed $\alpha_s/\alpha_{gr}$ for both Cases ① and ② .

In order to select better method among the Cases ① and ② , errors of the apparent thermal diffusivity is calculated by the following equation, and the results are shown in Fig. 2 for two typical

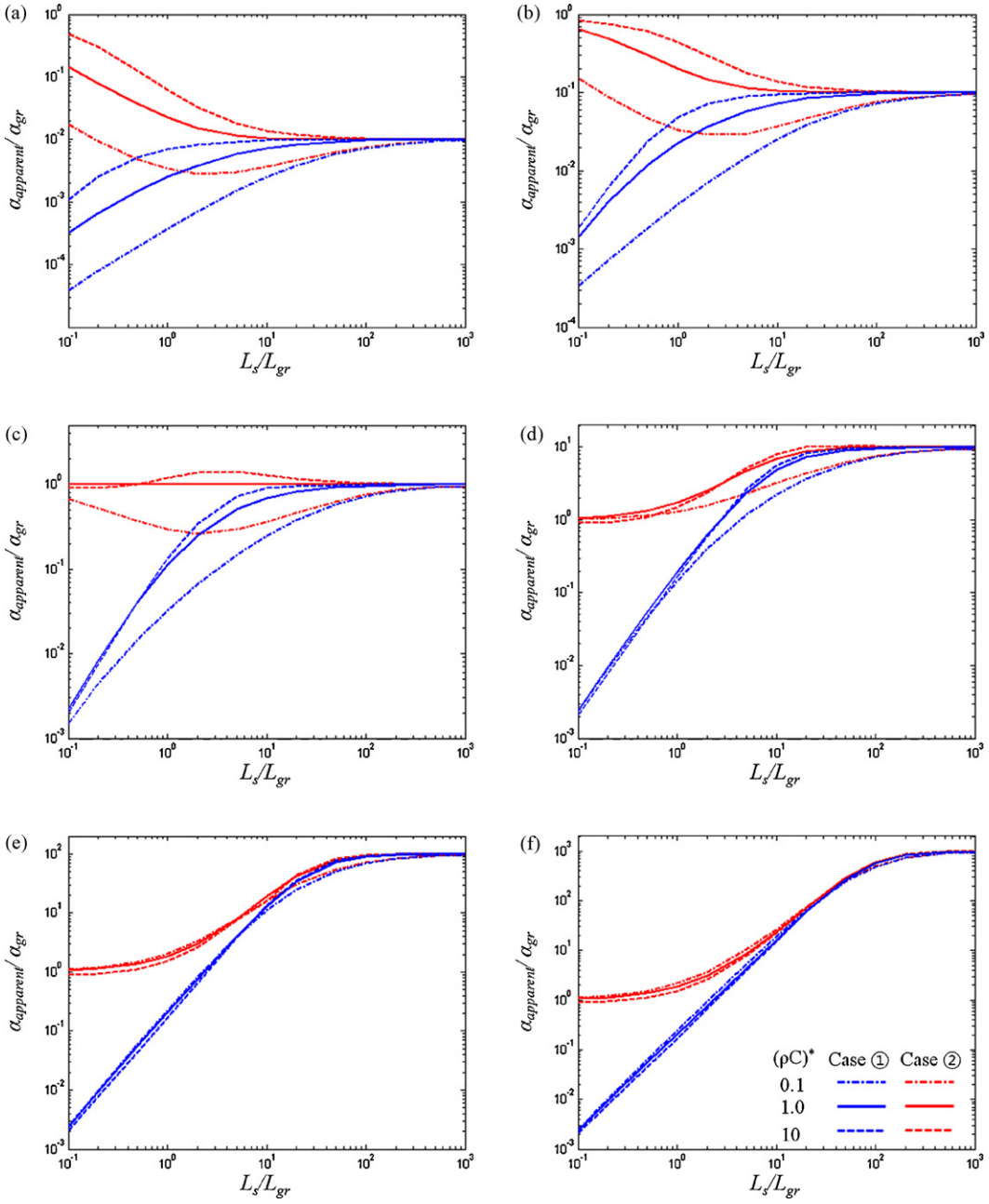


**Fig. 1.** Apparent thermal diffusivity of graphite-coated sample: (a) $\alpha^* = 0.01$, (b) $\alpha^* = 0.1$, (c) $\alpha^* = 1$, (d) $\alpha^* = 10$, (e) $\alpha^* = 100$ and (f) $\alpha^* = 1000$.

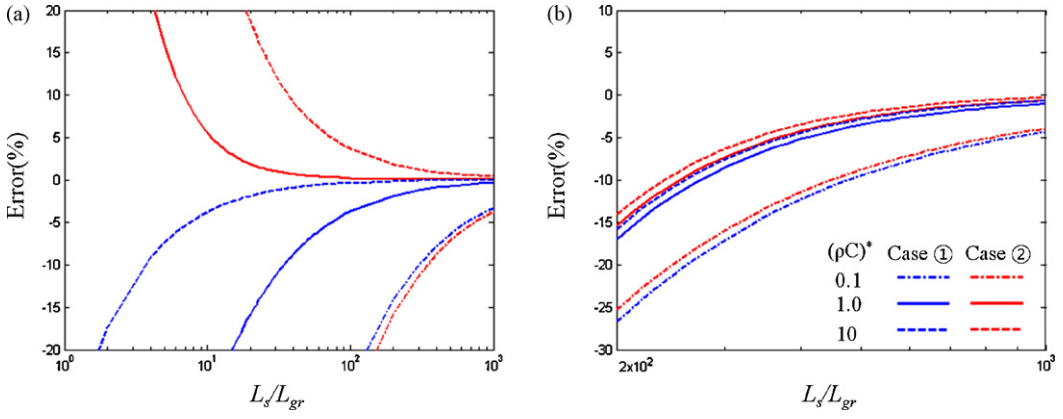


**Fig. 2.** Error of apparent thermal diffusivity of graphite-coated sample: (a) $\alpha^* = 0.01$ and (b) $\alpha^* = 1000$.

materials, $\alpha^* = 0.01$ and 1000.

$$\text{Error } (\%) = \frac{\alpha_{apparent} - \alpha_s}{\alpha_s} \times 100 \tag{4}$$

When $\alpha^*$ is less than one, Case ① underestimates the thermal diffusivity, and the error becomes large for small $L^*$ and $(\rho C)^*$, whereas the Case ② overestimates and the error is larger for small $L^*$ when $(\rho C)^*$ is equal to or greater than one. If $(\rho C)^*$ is less than one for Case ②, thermal diffusivity is usually underestimated. In order to find accurate thermal diffusivity when $(\rho C)^*$ is highly different from one, the sample must be sufficiently thick. For example, the thickness of the sample should be 1000 times greater than the graphite coating layer for $(\rho C)^* = 0.1$ and $\alpha^* = 0.01$ in Case ②.

On the other hand, when $\alpha^*$ is greater than one, both cases underestimate the thermal diffusivity. For this case, the error of Case ② is a little less than Case ① in the whole ranges of the thickness ratio and the specific thermal mass ratio. But such betterment is not appreciable. In other words, whether the graphite coating layer thickness is included or not, the 1-layer model can be used in very limited ranges of the ratios $\alpha^*$, $L^*$ and $(\rho C)^*$.

## 3. Theoretical formulations of the 1-layer and 3-layer models

In the real situation, the ideal conditions that lead to the simple result of Eq. (1) are not realizable. Due to physical constraints of the laser pulse generation equipment, it is impossible to generate width-less Dirac delta function pulse. The width of the pulse is always finite. And since the flash pulse transmits very intense heat on the sample surface, the flash method is always associated with radiation heat loss from the sample to surroundings. In addition, if the sample is coated with graphite on its surfaces, it causes delay of the response time and the measurement time becomes a little longer. Its effect becomes significant all the more when the sample temperature is high. Due to these limitations, Eq. (1) cannot be used for accurate measurement of thermal diffusivity. For a single layer of the test material only, Cape and Lehman [2] solved theoretically the unsteady heat conduction equation with appropriate boundary conditions and have developed a model to take account of the radiation heat losses on both the facial and radial surfaces. Their result is given by the following expression,

$$T(t) = \Delta T \sum_{m=0}^{\infty} P_m S_m \sum_{i=0}^{\infty} D_i(Y_r) \int_0^t W(\tau) \exp\left\{-\frac{\omega_{im}(t-\tau)}{\tau_0}\right\} d\tau$$
$$P_m = (-1)^m \frac{2\alpha}{L} \frac{S_m}{{S_m}^2 + 2Y_x + {Y_x}^2}$$
$$D_i(Y_r) = \frac{2Y_r}{{Y_r}^2 + z_i^2(Y_r)} \frac{1}{J_0(z_i)} \tag{5}$$
$$Y_r J_0(z_i) = z_i J_1(z_i)$$
$$\omega_{im} = -\left(\frac{L}{m}\right)^2 \left(\frac{{S_m}^2}{L^2} + \frac{z_i^2}{{r_0}^2}\right)$$

Here $T(t)$ is the rear surface temperature and $\Delta T = Q/C_t$ is the maximum temperature change of the sample; $Q$ is the total absorbed energy in the sample and $C_t$ is the total heat capacity of the sample. $S_m$ are the roots of the following equation:

$$({S_m}^2 - {Y_x}^2)\tan(S_m) - 2S_m Y_x = 0 \tag{6}$$

where $Y_x = 4\sigma\varepsilon_x {T_0}^3 k^{-1} L$, $Y_r = 4\sigma\varepsilon_r {T_0}^3 k^{-1} r_0$. $\sigma$ is the Stefan-Boltzmann constant and $\varepsilon$ is the total emissivity of the sample. $T_0$ is the sample temperature and $k$ is the thermal conductivity of the sample. $L$ is the thickness and $r_0$ is the radius of the sample. $\tau_0 = \alpha(L/\pi)^2$ is the characteristic heat diffusion time, $\alpha$ is the thermal diffusivity of the sample and $W(\tau)$ is the pulse shape function.

If the sample is relatively thin, the radial heat loss can be neglected. The basic equation that includes the heat loss effect through the facial surfaces only and the finite pulse time effect for the 1-layer model is obtained by simplifying Eq. (5). Cape and Lehmann [2] presented the following equation:

$$T(t) = \Delta T \sum_{m=0}^{\infty} A_m \int_0^t W(\tau) \exp\left\{-\left(\frac{S_m}{\pi}\right)^2 \frac{(t-\tau)}{\tau_0}\right\} d\tau \tag{7}$$

$$A_m = 2(-1)^m {S_m}^2 ({S_m}^2 + 2Y_x + {Y_x}^2)$$

For the layered composite materials such as electronic materials and materials which are resistant to wear, corrosion and heat, the analytical solution is more complicate due to the boundary conditions at the interfaces of the layers [18]. Heat loss effect can be taken account of by considering exponentially decreasing heat loss terms for layered materials. When the thermal resistance of the graphite coating layers at both sides is explicitly considered, the thermal flow path consists of graphite layer–test material–graphite layer and the 3-layer model for this case is given by Blumm et al. [19] as follows:

$$T(t) = \Delta T \left[1 + 2\sum_{m=1}^{\infty} \frac{\sum_{k=1}^{4} \omega_k X_k \int_0^t W(\tau) \exp\left\{-{\gamma_m}^2((t-\tau)/\eta_3)\right\} d\tau}{\sum_{k=1}^{4} \omega_k X_k \cos(\omega_k \gamma_m)}\right] \times \exp\left\{-\frac{\beta t}{2(L_1 + L_2 + L_3)}\right\} \tag{8}$$

$\omega = \eta_{1/3} + \eta_{2/3} + 1$, $\omega_2 = \eta_{1/3} + \eta_{2/3} - 1$
$\omega_3 = \eta_{1/3} - \eta_{2/3} + 1$, $\omega_4 = \eta_{1/3} - \eta_{2/3} - 1$
$X_1 = H_{1/3}\eta_{3/1} + H_{1/2}\eta_{2/1} + H_{2/3}\eta_{3/2} + 1$, $X_2 = H_{1/3}\eta_{3/1} - H_{1/2}\eta_{2/1} + H_{2/3}\eta_{3/2} - 1$
$X_3 = H_{1/3}\eta_{3/1} - H_{1/2}\eta_{2/1} - H_{2/3}\eta_{3/2} + 1$, $X_4 = H_{1/3}\eta_{3/1} + H_{1/2}\eta_{2/1} - H_{2/3}\eta_{3/2} - 1$
$H_i = \rho_i C_i L_i$, $\eta_i = L_i/\sqrt{\alpha_i}$ $(i = 1, 2 \text{ and } 3)$
$H_{i/j} = H_i/H_j$, $\eta_{i/j} = \eta_i/\eta_j$

This model also includes the radiation heat loss through the facial surfaces and the finite pulse time effect. In Eq. (7), $\rho_i$, $C_i$ and $L_i$ are density, specific heat and thickness of the $i$th layer of the sample and $\beta$ is the heat loss factor.

If the duration of the heating pulse is very small compared to its whole response time, $W(\tau)$ is assumed to be the Dirac delta function. To correct the effect of the finite duration time of the heating pulse, it is important to describe the shape of the pulse similarly with the actual pulse. The most suitable pulse shape for the laser or xenon flash is known as a modified exponential function [16] and it is expressed by

$$W(\tau) = \left\{1 - \exp\left(\frac{\tau}{s_1}\right)\right\} \exp\left(\frac{\tau}{s_2}\right) \quad (0 \le \tau \le t_e)$$
$$= \left\{1 - \exp\left(\frac{t_e}{s_1}\right)\right\} \exp\left(\frac{t_e}{s_2}\right) \exp\left\{\left(\frac{\tau - t_e}{s_3}\right)\right\} \quad (\tau \ge t_e) \tag{9}$$

Here $s_1$, $s_2$ and $s_3$ are time constants to adjust the pulse shape function to the actual pulse shape. Different pulse width, which is represented by $t_e$ in Eq. (9), is used according to the heat capacity and thermal diffusivity of the sample. In the present experiment that follows, they are 0.06, 0.18 and 0.31 ms. The integrals inEqs.

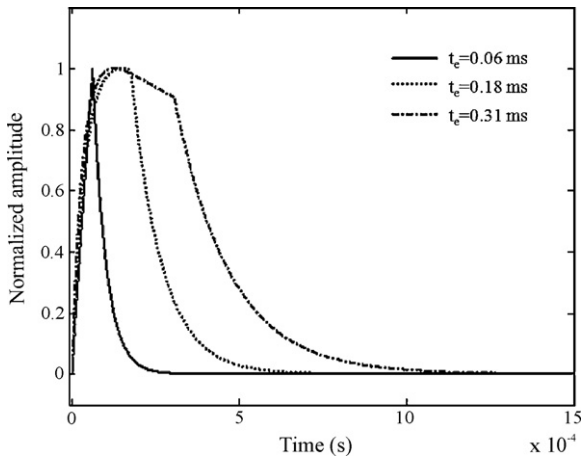


**Fig. 3.** Approximation of flash pulse shape for different values of pulse width.

(5), (7) and (8) are:

$$\int_0^t W(\tau)\exp\left\{-P(t-\tau)\right\}d\tau = \left[\frac{s_1}{Ps_1-1}\left[\exp\left\{\left(P-\frac{1}{s_1}\right)t_e\right\}-1\right]-\frac{s_1s_2}{Ps_1s_2-Ps_1-Ps_2}\left[\exp\left\{\left(P-\frac{1}{s_1}-\frac{1}{s_2}\right)t_e\right\}-1\right]\right]\exp(-Pt) + \frac{s_3}{Ps_3-1}\left\{1-\exp\left(\frac{t_e}{s_1}\right)\right\}\exp\left\{\left(\frac{1}{s_3}-\frac{1}{s_2}\right)t_e\right\}\left[\exp\left(-\frac{t}{s_1}\right)-\exp\left\{\left(P-\frac{1}{s_3}\right)t_e\right\}\exp(-Pt)\right] \quad (10)$$

Here $P$ is $(X_m/\pi)^2/\tau_0$ for the 1-layer model and ${\gamma_m}^2/\eta_3$ for the 3-layer model, respectively. It is important to choose an adequate pulse width to reduce uncertainties from the noise of the temperature rise curve at the rear surface of the sample. Fig. 3 shows a plot of Eq. (9) for different values of $t_e$.

## 4. Measurement of thermo-physical properties of graphite for use of 3-layer model

If the sample is relatively very thin or it is highly conductive so that the temperature rising time is very fast, the thermal resistance of the graphite coating layer is appreciable. In such cases, the 3-layer model that analyzes the conduction heat transfer through the 3-layer structure of graphite coating layer-test material-graphite coating layer is more appropriate to find the thermal diffusivity of the sample material. And in order to treat the graphite coating layer as a separate layer with the 3-layer model, homogeneity in the graphite coating layer must be confirmed. In this study, Graphit 33 (Kontakt Chemie, Germany) was used here to stack the graphite coating layer by spraying. The SEM photographs of the graphite coating layer are shown in Fig. 4. The structure consists of graphite grains and pores. Even though the structure is locally heterogeneous, since the size of the grains is very small compared with the thickness of the coating layer, an average thermal diffusivity can be assumed [20–22]. Araki et al. [22] suggested that if there are

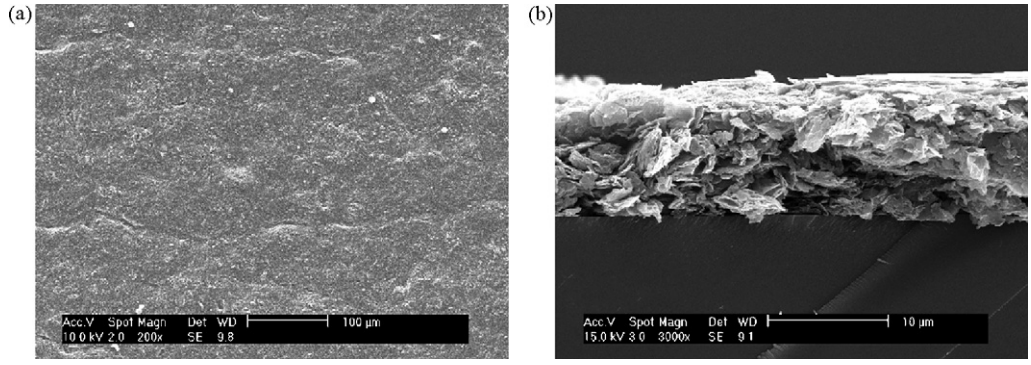


**Fig. 4.** SEM photographs of graphite coating layer: (a) front view and (b) cross-sectional view.

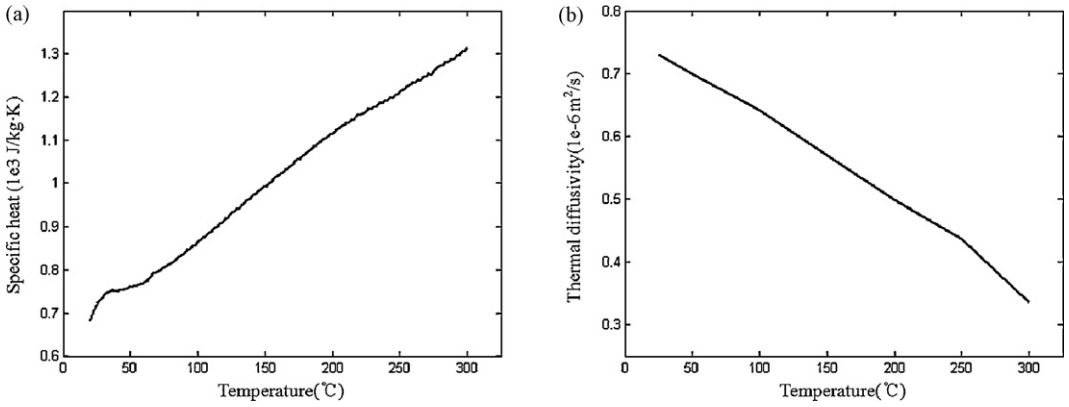


**Fig. 5.** Thermophysical properties of graphite coating layer: (a) specific heat and (b) thermal diffusivity.

more than 10 grains stacked in the thickness-wise heat flow direction over the whole plane, the thermal resistance in that direction may be considered homogeneous. A number of samples have been made and it was found that the range of the coating layer thickness was 5–15 μm with an average value of about 10 μm. Average size of the graphite grains is about 2–3 μm long and 0.5 μm thick and about 20 graphite grains are stacked thickness-wise. Therefore the thermal resistance of the coating layer in the heat-flow direction may be considered homogeneous over the present sample surface.

In this study, a graphite sample of uniform thickness of 0.65 mm was formed by spraying, and the flash method was used to measure the thermal diffusivity of the one graphite layer. Specific heat of the graphite layer was measured by DSC (differential scanning calorimetry). The measurements were carried out in a temperature range of 25–300 °C. Bulk density at 25 °C was 509.3 kg m$^{-3}$. Measured specific heat and thermal diffusivity are shown in Fig. 5.

## 5. Experimental measurement

In this section, four typical thin solid materials are selected and their thermal diffusivities are calculated, and their measurement accuracies are to be compared. Since the comparison requires accurate reference value of the sample's thermal diffusivity, they are measured first by the 1-layer model using Eq. (5). The materials selected for this study are copper, aluminum, iron and Inconel 600. Their specific heat and density in the temperature range 25–300 °C are tabulated in Table 1.

As already discussed in Section 2, in order to use the 1-layer model to find out the thermal diffusivity as accurate as possible, the sample must have an adequate thickness that allows the accurate measurement. Based on the thermal diffusivity in Ref. [17], the error in the apparent thermal diffusivity of graphite-coated samples is calculated theoretically as a function of the thickness ratio $L_s/L_{gr}$, and Case ① is used here, and the results are shown in Fig. 6. From this study, it is found out that the minimum thickness ratio $L_s/L_{gr}$ that yields less than 5% error are 147, 134, 61, 29 for copper, aluminum, iron and Inconel 600, respectively. Therefore, based on the graphite coating thickness of about 10 μm, the sample thicknesses for measuring the accurate reference thermal diffusivities of copper, aluminum, iron and Inconel 600 are determined to be 2.997, 2.998, 2.004 and 1.998 mm, respectively, that are sufficiently larger than the required minimum thickness. The thin sample materials are coated at both sides with graphite and their dimensions are listed in Table 2.

The analysis model equations used to find the thermal diffusivities of the selected thin materials are Eq. (7) for the 1-layer model and Eq. (8) for the 3-layer model. Correction for the heat loss through the facial surfaces only is taken account of in both models because all samples are relatively thin as shown in Table 2. On the other hand, in order to appreciate the effect of the finite pulse time, the finite pulse time is either corrected or not in both models. Finally the sample thickness is considered for the 1-layer model in two ways as Cases ① and ② in Eq. (3). In the experiment, the laser pulse is applied to the graphite-coated front surface and the temperature at the graphite-coated rear surface is recorded as a function of time. Then the recorded temperature rise curve is fitted to the model equations by adjusting the thermal diffusivity. The measured thermal diffusivity of the graphite coating in Section 4 was used in the model equations. Here, the curve-fitting was carried by using the nonlinear parameter estimation of Levenberg–Marquardt algorithm [23]. Eqs. (7) and (8) are re-written as $\vec{Y} = \eta(\vec{X}, \vec{\phi}) + \vec{\varepsilon}$ for nonlinear parameter estimation where the independent variable $\vec{X}$ is time t, measured variable $\vec{Y}$ is $T$ at time $t$ with additive error $\vec{\varepsilon}$. The dependent variables that are parameters to be estimated are $\Delta T$, $\alpha$ and $Y_x$ in Eq. (7) for the 1-layer model for given sample thickness $L$ and $\Delta T$, $\alpha_2$ and $\beta$ in Eq. (8) for the 3-layer model for given sample thickness and specific thermal mass $L_i$, $(\rho C)_i$ ($i = 1, 2, 3$) and thermal diffusivity $\alpha_1$, $\alpha_3$, respectively. A temperature rise curve is obtained by calculating $T$ at 1800 temporal points on the time axis. Summarizing, the models used in the present work are listed as follows:

i. 1-Layer model without finite pulse time correction (Case ① ).
ii. 1-Layer model with finite pulse time correction (Case ① ).
iii. 1-Layer model without finite pulse time correction (Case ② ).

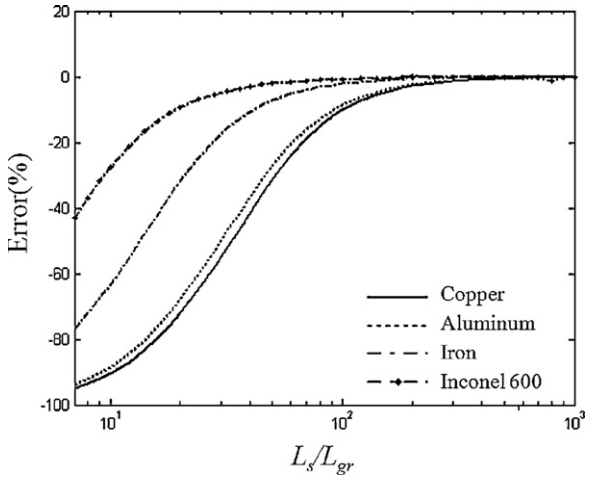


**Fig. 6.** Theoretical error of the thermal diffusivity of the graphite-coated samples (at 25 °C).

**Table 1**
Specific heat and density of the selected materials [17].

| Temperature (°C) | Copper | | Aluminum | | Iron | | Inconel 600 | |
|---|---|---|---|---|---|---|---|---|
| | $C_p$ (J kg$^{-1}$ K$^{-1}$) | Density (kg m$^{-3}$) | $C_p$ (J kg$^{-1}$ K$^{-1}$) | Density (kg m$^{-3}$) | $C_p$ (J kg$^{-1}$ K$^{-1}$) | Density (kg m$^{-3}$) | $C_p$ (J kg$^{-1}$ K$^{-1}$) | Density (kg m$^{-3}$) |
| 25 | 388 | 8890 | 882 | 2700 | 450 | 7870 | 444 | 8340 |
| 100 | 397 | 8874 | 911 | 2693 | 478 | 7863 | 467 | 8271 |
| 200 | 407 | 8858 | 959 | 2686 | 523 | 7845 | 489 | 8320 |
| 300 | 411 | 8841 | 1009 | 2678 | 562 | 7815 | 503 | 8306 |

**Table 2**
Thickness of the thin samples and coating layers.

| Thickness | Copper | Aluminum | Iron | Inconel 600 |
|---|---|---|---|---|
| $L_{gr}$ (mm) | 0.0085 | 0.008 | 0.008 | 0.011 |
| $L_s$ (mm) | 0.503 | 0.484 | 0.199 | 0.101 |
| $L^*$ | 59.18 | 60.5 | 24.88 | 9.18 |

**Table 3**
Experimentally determined thermal diffusivity of the selected materials.

| | Thermal diffusivity (1E−6 $m^2 s^{-1}$) | | | Temperature (°C) | | | |
|---|---|---|---|---|---|---|---|
| | | | | 25 | 100 | 200 | 300 |
| Copper | 1-Layer ($L$ = 0.503 mm) | Case ① | Pulse not corrected | 60.362 ± 0.574 | 58.136 ± 0.545 | 54.604 ± 0.284 | 51.457 ± 0.261 |
| | | | Pulse corrected | 83.457 ± 1.061 | 79.604 ± 1.032 | 73.349 ± 0.467 | 67.838 ± 0.384 |
| | | Case ② | Pulse not corrected | 64.511 ± 0.614 | 62.132 ± 0.583 | 58.357 ± 0.303 | 54.994 ± 0.279 |
| | | | Pulse corrected | 89.168 ± 1.133 | 85.053 ± 1.102 | 78.616 ± 0.502 | 72.507 ± 0.410 |
| | 3-Layer ($L$ = 0.503 mm) | | Pulse not corrected | 76.013 ± 0.466 | 75.888 ± 0.958 | 74.120 ± 0.636 | 74.036 ± 0.772 |
| | | | Pulse corrected | 116.756 ± 0.059 | 111.802 ± 0.125 | 106.964 ± 0.162 | 104.008 ± 0.001 |
| | Thick sample ($L$ = 2.997 mm) | | | 113.078 ± 1.069 | 109.661 ± 0.762 | 104.775 ± 0.355 | 100.732 ± 0.580 |
| Aluminum | 1-Layer ($L$ = 0.484 mm) | Case ① | Pulse not corrected | 52.808 ± 0.268 | 50.802 ± 0.331 | 47.063 ± 0.322 | 44.886 ± 0.449 |
| | | | Pulse corrected | 71.396 ± 0.457 | 67.948 ± 0.551 | 61.455 ± 0.582 | 57.918 ± 0.278 |
| | | Case ② | Pulse not corrected | 57.263 ± 0.290 | 55.088 ± 0.359 | 51.033 ± 0.349 | 48.672 ± 0.487 |
| | | | Pulse corrected | 77.395 ± 0.495 | 73.660 ± 0.597 | 66.629 ± 0.636 | 62.738 ± 0.412 |
| | 3-Layer ($L$ = 0.484 mm) | | Pulse not corrected | 64.121 ± 0.380 | 62.443 ± 0.578 | 61.595 ± 0.605 | 62.864 ± 0.697 |
| | | | Pulse corrected | 90.919 ± 0.196 | 88.427 ± 0.126 | 84.988 ± 0.031 | 83.109 ± 0.135 |
| | Thick sample ($L$ = 2.998 mm) | | | 90.846 ± 0.643 | 88.387 ± 0.472 | 84.960 ± 0.346 | 82.568 ± 0.049 |
| Iron | 1-Layer ($L$ = 0.199 mm) | Case ① | Pulse not corrected | 12.007 ± 0.115 | 10.948 ± 0.050 | 9.339 ± 0.076 | 8.099 ± 0.085 |
| | | | Pulse corrected | 14.098 ± 0.094 | 12.454 ± 0.253 | 10.463 ± 0.107 | 8.892 ± 0.101 |
| | | Case ② | Pulse not corrected | 14.015 ± 0.134 | 12.780 ± 0.058 | 10.901 ± 0.089 | 9.454 ± 0.100 |
| | | | Pulse corrected | 16.444 ± 0.144 | 14.574 ± 0.274 | 12.217 ± 0.108 | 10.347 ± 0.135 |
| | 3-Layer ($L$ = 0.199 mm) | | Pulse not corrected | 14.536 ± 0.426 | 13.412 ± 0.099 | 11.656 ± 0.182 | 10.497 ± 0.147 |
| | | | Pulse corrected | 17.840 ± 0.251 | 16.278 ± 0.128 | 13.807 ± 0.140 | 12.043 ± 0.202 |
| | Thick sample ($L$ = 2.004 mm) | | | 18.433 ± 0.190 | 16.238 ± 0.131 | 14.111 ± 0.090 | 11.934 ± 0.052 |
| Inconel 600 | 1-Layer ($L$ = 0.101 mm) | Case ① | Pulse not corrected | 2.168 ± 0.009 | 2.078 ± 0.014 | 2.002 ± 0.014 | 1.894 ± 0.018 |
| | | | Pulse corrected | 2.404 ± 0.012 | 2.285 ± 0.013 | 2.190 ± 0.017 | 2.064 ± 0.023 |
| | | Case ② | Pulse not corrected | 3.215 ± 0.013 | 3.082 ± 0.021 | 2.969 ± 0.021 | 2.809 ± 0.027 |
| | | | Pulse corrected | 3.565 ± 0.016 | 3.391 ± 0.014 | 3.249 ± 0.025 | 3.058 ± 0.032 |
| | 3-Layer ($L$ = 0.101 mm) | | Pulse not corrected | 2.994 ± 0.011 | 3.043 ± 0.026 | 3.190 ± 0.033 | 3.307 ± 0.031 |
| | | | Pulse corrected | 3.501 ± 0.024 | 3.589 ± 0.025 | 3.813 ± 0.032 | 4.056 ± 0.038 |
| | Thick sample ($L$ = 1.998 mm) | | | 3.517 ± 0.035 | 3.664 ± 0.017 | 3.887 ± 0.019 | 4.144 ± 0.022 |

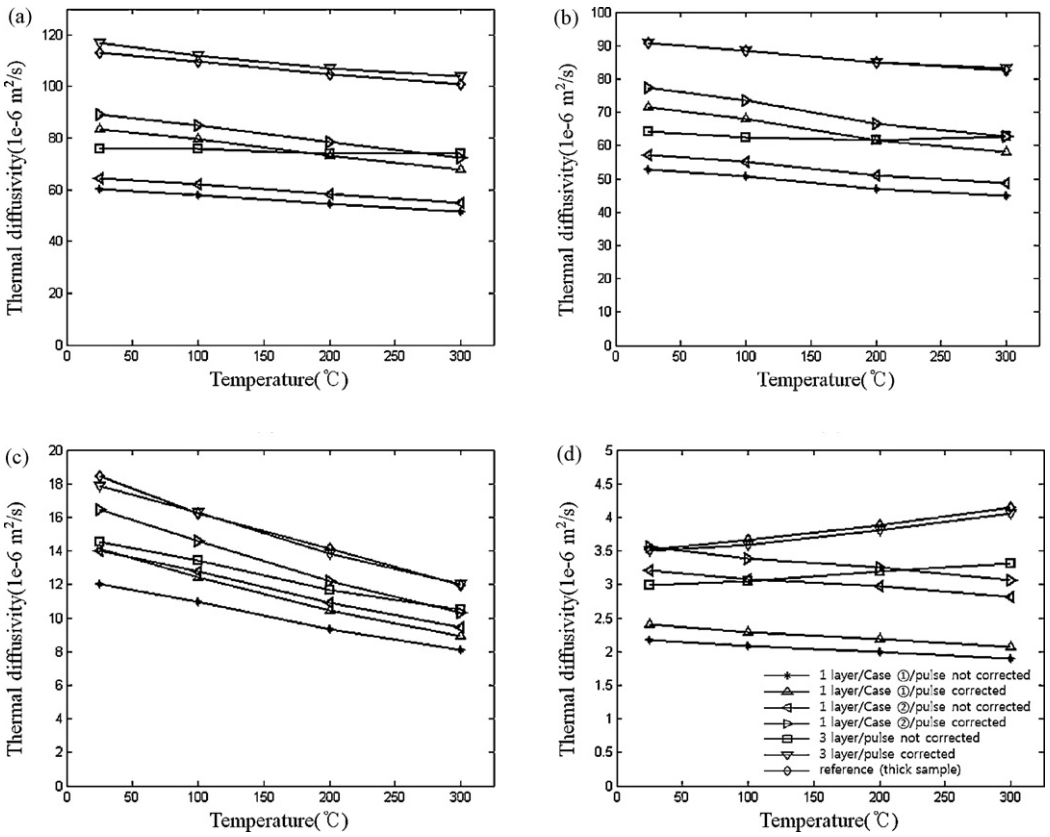


**Fig. 7.** Thermal diffusivity of the selected materials: (a) copper ($L$ = 0.503 mm), (b) aluminum ($L$ = 0.484 mm), (c) iron ($L$ = 0.199 mm) and (d) Inconel 600 ($L$ = 0.101 mm).

**Table 4**
Error of measured thermal diffusivity of the selected materials.

| | Error (%) | | | Temperature (°C) | | | |
|---|---|---|---|---|---|---|---|
| | | | | 25 | 100 | 200 | 300 |
| Copper ($L$ = 0.503 mm) | 1-Layer | Case ① | Pulse not corrected | −46.619 | −46.986 | −47.884 | −48.917 |
| | | | Pulse corrected | −26.195 | −27.409 | −29.994 | −32.655 |
| | | | Theoretical | −24.560 | −28.386 | −32.238 | −36.733 |
| | | Case ② | Pulse not corrected | −42.950 | −43.342 | −44.302 | −45.406 |
| | | | Pulse corrected | −21.145 | −22.440 | −24.967 | −28.020 |
| | | | Theoretical | −19.375 | −23.464 | −27.581 | −32.385 |
| | 3-Layer | | Pulse not corrected | −32.779 | −30.798 | −29.258 | −26.502 |
| | | | Pulse corrected | 3.252 | 1.952 | 2.089 | 3.252 |
| Aluminum ($L$ = 0.484 mm) | 1-Layer | Case ① | Pulse not corrected | −41.871 | −42.523 | −44.606 | −45.638 |
| | | | Pulse corrected | −21.410 | −23.124 | −27.665 | −29.854 |
| | | | Theoretical | −20.237 | −23.706 | −27.326 | −31.587 |
| | | Case ② | Pulse not corrected | −36.967 | −37.675 | −39.933 | −41.052 |
| | | | Pulse corrected | −14.806 | −16.663 | −21.576 | −24.018 |
| | | | Theoretical | −14.877 | −18.579 | −22.442 | −26.989 |
| | 3-Layer | | Pulse not corrected | −29.418 | −29.353 | −27.501 | −23.865 |
| | | | Pulse corrected | 0.081 | 0.045 | 0.034 | 0.654 |
| Iron ($L$ = 0.199 mm) | 1-Layer | Case ① | Pulse not corrected | −34.862 | −32.575 | −33.821 | −32.133 |
| | | | Pulse corrected | −23.516 | −23.304 | −25.857 | −25.491 |
| | | | Theoretical | −23.752 | −25.737 | −27.352 | −28.761 |
| | | Case ② | Pulse not corrected | −23.967 | −21.297 | −22.751 | −20.781 |
| | | | Pulse corrected | −10.790 | −10.245 | −13.428 | −13.297 |
| | | | Theoretical | −10.998 | −13.315 | −15.200 | −16.845 |
| | 3-Layer | | Pulse not corrected | −21.141 | −17.401 | −17.397 | −12.037 |
| | | | Pulse corrected | −3.217 | 0.248 | −2.154 | 0.911 |
| Inconel 600 ($L$ = 0.101 mm) | 1-Layer | Case ① | Pulse not corrected | −38.366 | −43.287 | −48.500 | −54.293 |
| | | | Pulse corrected | −31.647 | −37.635 | −43.646 | −50.205 |
| | | | Theoretical | −31.809 | −37.035 | −43.342 | −50.057 |
| | | Case ② | Pulse not corrected | −8.591 | −15.894 | −23.621 | −32.212 |
| | | | Pulse corrected | 1.352 | −7.450 | −16.422 | −26.215 |
| | | | Theoretical | 1.133 | −6.617 | −15.971 | −25.929 |
| | 3-Layer | | Pulse not corrected | −14.879 | −16.950 | −17.911 | −20.186 |
| | | | Pulse corrected | −0.452 | −2.049 | −1.883 | −2.115 |

iv. 1-Layer model with finite pulse time correction (Case ② ).
v. 3-Layer model without finite pulse time correction.
vi. 3-Layer model with finite pulse time correction.

The temperature range in the experiment was 25–300 °C. The determined thermal diffusivities with 95% confidence interval and the errors of the six models listed above are presented in Fig. 7 and Tables 3 and 4. The errors are calculated based on the reference values measured with thick samples.

When one compares the results of the models (i vs. ii, iii vs. iv and v vs. vi), it is observed in Table 4 that correction of finite pulse time effect reduces the errors significantly for the thin and highly conductive metal samples. Next, effect of including the thickness of the graphite coating layer in the 1-layer model is scrutinized by comparing the results of Cases ① and ② . As can be seen, Case ② helps to reduce the error of the thermal diffusivity slightly compared to Case ① . When the finite pulse time effect is corrected, Case ② improves the accuracy by about 5, 7, 13 and 33% than Case ① for copper, aluminum, iron, and Inconel 600, respectively at 25 °C. The 1-layer model with finite pulse time correction evaluates the thermal diffusivity up to about 33 and 28% error for Cases ① and ②, respectively, the largest value for copper at 300 °C. On the other hand, thermal diffusivity determined by the pulse corrected 3-layer model is much more accurate than such 1-layer model. Errors are up to about 3.3% in the whole temperature range for all materials studied in the present study. Therefore, it is concluded that the 3-layer model with pulse correction is the best one among the six models to determine thermal diffusivity for the thin samples. Note that in this case thermophysical properties of the coating layer must be known as accurate as possible.

## 6. Conclusions

The present study was carried out to improve the flash method that is used to measure the thermal diffusivity of graphite-coated thin specimens. In the first part, assuming that the graphite-coated sample is a single layer of uniform material, apparent thermal diffusivity has been defined and the variation of the apparent thermal diffusivity for a number of different materials was theoretically calculated as a function of thickness ratio $L_s/L_{gr}$ between the sample and the graphite coating layer with the specific thermal mass ratio $(\rho C)_s/(\rho C)_{gr}$ as another parameter. As a result, it was found that the apparent thermal diffusivity deviates appreciably from the true thermal diffusivity when the material's thermal diffusivity is high and sample thickness is thin compared to the coating layer thickness, or when the material's specific thermal mass is relatively small. In such a case, a better mathematical model for the flash method is required. From this study, one can find the minimum thickness ratio $L_s/L_{gr}$ for the apparent thermal diffusivity method to be accurate enough to measure the graphite-coated sample's thermal diffusivity within a predetermined error range.

Secondly, the measurement accuracy by the 1-layer model and 3-layer model was investigated. In these models, the radiation heat loss effect is included. And accuracy improvement by including the effect of the finite pulse width was also scrutinized. In the 1-layer model, neglecting the effect of the presence of the graphite coating layers, the graphite-coated sample is assumed as a single layer of the sample material. In contrast, the 3-layer model treats the graphite coating layers at both sides of the sample surfaces in the best way. The model equation for the 1-layer model is that of Cape and Lehman [2], and that for the 3-layer model is Blumm et al.'s solution [19]. In order to use the 3-layer model, the thermophysical properties of the graphite coating layer have been measured in this study. A total of six different methods were used to measure the thermal diffusivities of copper, aluminum, iron, and Inconel 600 in a temperature range of 25–300 °C and their measurement accuracies were compared. It was found that error of the 1-layer model with the finite pulse width correction is up to about 33% with largest value for copper at 300 °C. In contrast, the 3-layer model with the finite pulse width correction yields the measurement error of up to about 3.3% with largest error for copper at 300 °C. As a conclusion, the 3-layer model with the finite pulse width correction is the most accurate model for measurement of thin graphite-coated samples.

## References

[1] W.J. Parker, R.J. Jenkins, C.P. Butler, G.L. Abbott, J. Appl. Phys. 32 (1961) 1679–1684.
[2] J.A. Cape, G.W. Lehman, J. Appl. Phys. 34 (1963) 1909–1913.
[3] J. Blumm, J. Opfermann, High Temp. High Press. (2002) 515–521.
[4] R.D. Cowan, J. Appl. Phys. 34 (1963) 926–927.
[5] A. Cezairliyan, T. Baba, R. Taylor, Int. J. Thermophys. 15 (1994) 317–341.
[6] K. Beedham, I.P. Dalrymple, Rev. Int. Hautes Temp. Refract. 7 (1970) 278–283.
[7] J.A. McKay, J.T. Schrempf, J. Appl. Phys. 47 (1967) 1668–1671.
[8] ISO/DIS 18755.
[9] A.P.F. Albers, T.A.G. Restivo, L. Pagano, J.B. Baldo, Thermochim. Acta 370 (2001) 111–118.
[10] N. Araki, A. Makino, J. Mihara, Int. J. Thermophys. 13 (1992) 331–348.
[11] J.D. Guo, G.H. He, Y.Y. Zhang, et al., Int. J. Thermophys. 21 (2000) 479–485.
[12] F. Cernuschi, L. Lorenzoni, P. Bianchi, A. Figari, Infrared Phys. Technol. 43 (2002) 133–138.
[13] S.K. Kim, Y.J. Kim, Thermochim. Acta 468 (2008) 6–9.
[14] K.B. Larson, K. Koyama, J. Appl. Phys. 38 (1967) 465–474.
[15] R.E. Taylor, J.A. Cape, Appl. Phys. Lett. 5 (1964) 212–213.
[16] NETZSCH-LFA HELP.
[17] Y.S. Touloukian, R.W. Powell, C.Y. Ho, P.G. Klemens, Thermophysical Properties of Matter, Plenum, New York, 1970.
[18] H.J. Lee, Purdue University, Ph.D. Thesis, 1975.
[19] J. Blumm, J. Opfermann, T. Matsui, Thermophys. Prop. 24 (2003) 396–398.
[20] J.F. Kerrisk, J. Appl. Phys. 42 (1971) 267–271.
[21] H.J. Lee, R.E. Taylor, J. Appl. Phys. 47 (1967) 148–151.
[22] N. Araki, D.W. Tang, A. Makino, M. Hashimoto, T. Sano, Int. J. Thermophys. 19 (1998) 1239–1251.
[23] D. Marquardt, SIAM J. Appl. Math. 11 (1963) 431–441.